3D parallel computation for transportation of gravel particles due to downward water jets

Hirofumi Yanagi[1], Daisuke Toriu[2], Satoru Ushijima[2 *]

[1]Graduate School of Engineering, Kyoto University
[2]Academic Center for Computing and Media Studies, Kyoto University

*ushijima.satoru.3c@kyoto-u.ac.jp

Abstract. 3D parallel computations with a multiphase model were performed for the transportation of gravel particles due to downward water jets. In the computations, the gravel particle models have 26 different shapes determined with non-spherical actual gravel particles. Compared with the experimental results, it was shown that the predicted gravel bed heights are in good agreement with the measured results. In addition, the vorticity distributions and coarse-grained fluid forces acting on the gravel particles were numerically visualized to consider the mechanism of the transportation of the gravel particles.

Keywords: Parallel computation, Multiphase model, Downward water jet, Particle transportation

1. Introduction

To numerically predict the transportation of sand and gravel particles due to water flows, it is important to consider fluid-solid mechanical interactions and contacts among particles. Aman et al. [1], for example, have performed direct numerical simulations for transportation of spherical sediment particles and pattern formation over an erodible bed. However, the shapes of the particles are also necessary to be considered in the numerical simulation since the actual sediment particles have complicated shapes.

In this study, a multiphase model [2] is applied to the experiments for transportation of gravel particles due to downward water jets. The gravel particle models used in the computation have 26 different shapes determined with non-spherical actual gravel particles [2] to consider effects of their shapes. The numerical results of gravel bed heights are compared with the experimental results and the vorticity in the fluid and coarse-grained fluid forces are calculated to discuss the transportation mechanism of gravel particles.

2. Numerical method

The present model [2] based on MAC method deals with the multiphase field consisting of fluid and solid phases, where each phase is assumed to be incompressible and immiscible.

The governing equations are given by the following incompressible condition, mass and momentum equations:

$$\frac{\partial u_j}{\partial x_j} = 0 \tag{1}$$

$$\frac{\partial \rho}{\partial t} + \frac{\partial}{\partial x_j}(\rho u_j) = 0 \tag{2}$$

$$\frac{\partial u_i}{\partial t} + \frac{\partial}{\partial x_j}(u_i u_j) = g_i - \frac{1}{\rho}\frac{\partial p}{\partial x_i} + \frac{1}{\rho}\frac{\partial}{\partial x_j}\left[\mu\left(\frac{\partial u_i}{\partial x_j} + \frac{\partial u_j}{\partial x_i}\right)\right] \tag{3}$$

where t is time, x_i is the i-th component of three-dimensional orthogonal coordinates and g_i is the acceleration of external force. While the velocity component u_i is the mass-averaged value in the mixture of fluids, volume-averaged variables are used for density ρ, pressure p and viscous coefficient μ. The governing equations are discretized with a finite volume method on collocated-grid system. The number of processes in parallel computations is 272 with flat MPI using supercomputer system (Xeon Broadwell, 18 cores 2.1 GHz × 2 / node) in Kyoto University. The gravel particle models are assumed to be rigid bodies. The models have 26 different shapes each of which is determined from the 500 actual particles as shown in Fig. 1. The numbers of each model used in computations are determined from the measured proportions of those to the 500 actual particles [2]. The particles models are represented by multiple tetrahedron elements as shown in Fig. 2 (a). The fluid forces acting on gravel particles are estimated from the volume integral of the pressure and viscosity terms without empirical coefficients, such as drag coefficient. On the other hand, the contact forces among gravel particle models are estimated on the basis of a distinct element method (DEM) [3] using multiple contact-detection spheres as shown in Fig. 2 (b).

3. Results and discussion

The experimental and calculation areas are shown in Fig. 3. Figure 4 and Figure 5 show the distributions of gravel particles due to downward water jets. Figure 4 shows the distributions only in the range of $0 \leq x_2 \leq 32$ [mm] so as to easily view the scoured shapes of the gravel bed. As shown in Fig. 4 and Fig. 5, the gravel particles are transported just below the inflow port and the gravel particle layer is largely scoured. Figure 6 shows comparisons

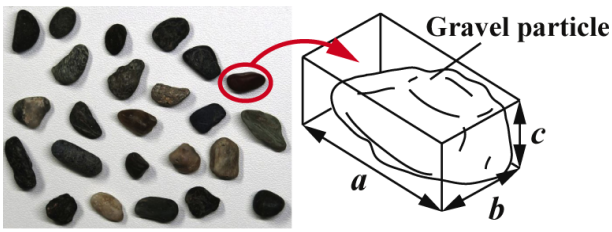

Figure 1: Actual gravel particles and three axes (a, b and c) for determination of the particle models [2]

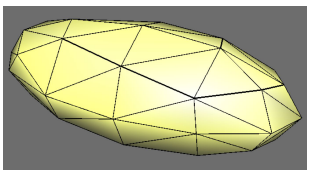

(a) Multiple tetrahedron elements [2]

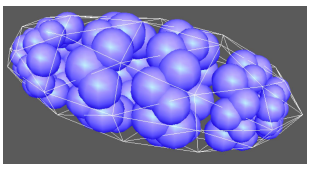

(b) Contact-detection spheres [2]

Figure 2: Gravel particle model

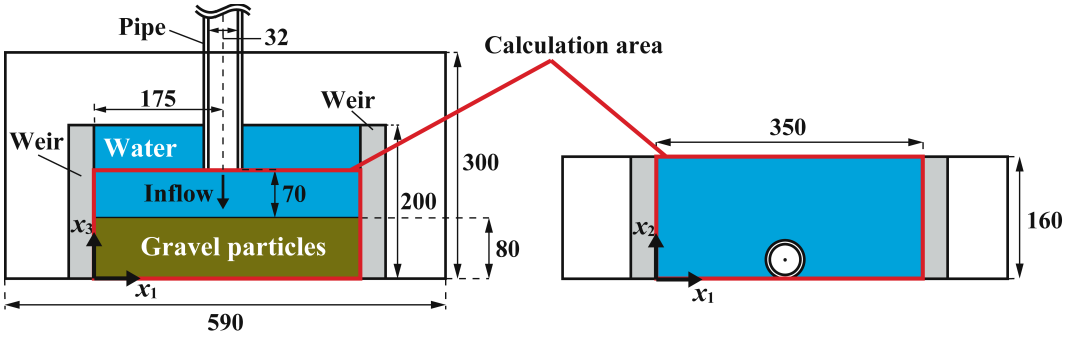

Figure 3: Experimental and calculation areas (unit [mm], left: side view, right: plan view)

of gravel bed heights in steady states between the calculated and experimental results. The experiments were conducted twice (case1, case2) with different initial distributions of the gravel particles. The error bars in Fig. 6 indicate the mean diameter of b (7.05 [mm]). As shown in Fig. 6, slightly differences can be seen between the calculated and experimental results. However, the differences are approximately equal the mean diameter of b. Thus, it can be concluded that the reasonable results are obtained.

Figure 7 shows the intensity of vorticity vectors in $x_1 - x_3$ plane on $x_2 = 0.012$ [m] and $x_2 - x_3$ plane on $x_1 = 0.80$ [m] at $t = 3.35$ [s]. The gravel particles are shown in $0.008 \leq x_2 \leq 0.016$ [m] and $0.784 \leq x_1 \leq 0.816$ [m] with only white color. In addition, Fig. 8 shows the distribution of coarse-grained fluid forces in same planes and time as those in Fig. 7. As shown in Fig. 7, the intensity of vorticity vectors became large around the surface of the scour hole except for just below the inflow port. By contrast, the large intensity of coarse-grained fluid force vectors was seen just below the inflow port as shown in Fig. 8. Hence, it is concluded that the local scour is developed by the spreading flow in the radial directions from just below the inflow port, where the large intensity of coarse-grained fluid force vectors is predicted.

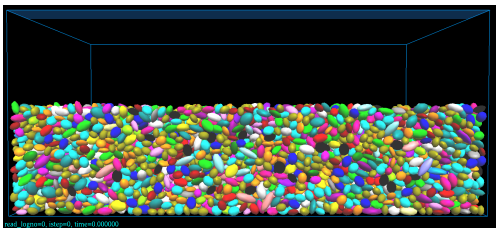

(a) $t = 0.0$ [s]

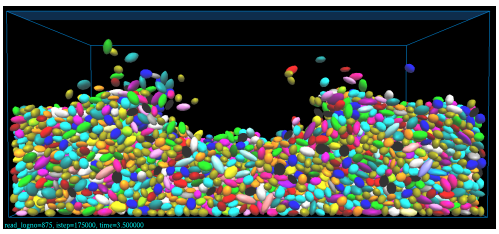

(b) $t = 3.5$ [s]

Figure 4: Distributions of gravel particles by computation (in $0 \leq x_2 \leq 32$ [mm])

(a) $t = 0.0$ [s]

(b) $t = 3.5$ [s]

Figure 5: Distributions of gravel particles by experiments

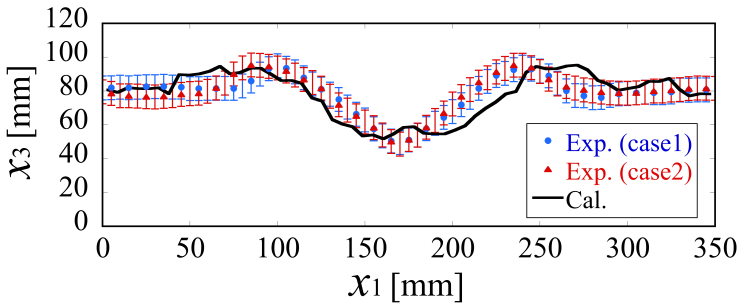

Figure 6: Gravel bed heights between computation and experiments in steady states

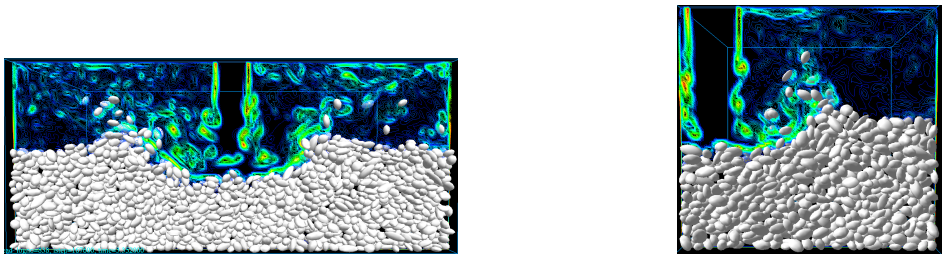

(a) $x_1 - x_3$ plane on $x_2 = 0.012$ [m] (b) $x_2 - x_3$ plane on $x_1 = 0.80$ [m]

Figure 7: Intensity of vorticity vectors, $t = 3.35$ [s]

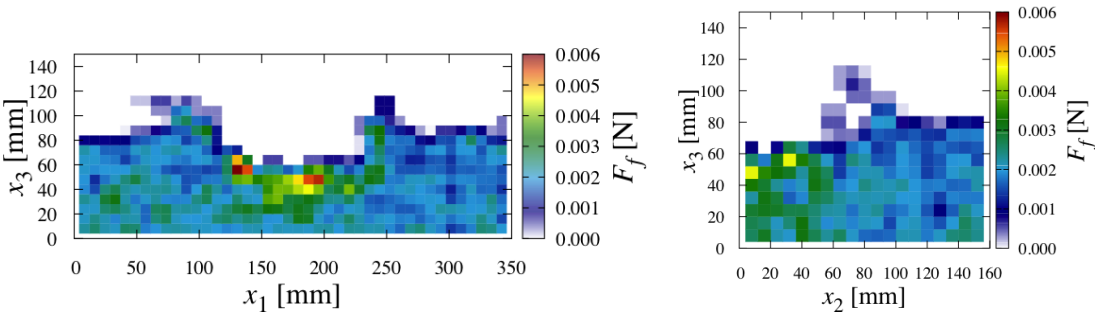

(a) $x_1 - x_3$ plane on $x_2 = 0.012$ [m] (b) $x_2 - x_3$ plane on $x_1 = 0.80$ [m]

Figure 8: Distribution of coarse-grained fluid forces, $t = 3.35$ [s]

References

[1] A. G. Kidanemariam, M. Uhlmann: Direct numerical simulation of pattern formation in subaqueous sediment, *Journal of Fluid Mechanics*, 750, (2014), R2.

[2] S. Ushijima, D. Toriu, H. Yanagi: Multiphase model to predict many gravel particles transported by free-surface flows (in press), *CMFF'18*, (2018).

[3] P. A. Cundall, O. D. L. Strack: A discrete numerical model for granular assemblies, *Geotechnique*, 29:1 (1979), 47–65.